RSC Advances

ROYAL SOCIETY OF CHEMISTRY

www.rsc.org/advances

Revealing the Mechanism of *Melia Toosendan* Fruit-Induced Liver Injury in Mice by Integrating microRNA and mRNA-Based Toxicogenomics data

Cai Ji[a#], Jie Zheng[a#], Wei Tong[a], Xiaoyan Lu[a], Xiaohui Fan[a]*, Yue Gao[b]*

[a] Pharmaceutical Informatics Institute, College of Pharmaceutical Sciences, Zhejiang University, Hangzhou 310058, China

[b]Department of Pharmacology and Toxicology, Beijing Institute of Radiation Medicine, Beijing 100850, China.

[#] the authors contributed equally to this study.

Correspondence should be addressed to Dr. Xiaohui Fan (E-mail:fanxh@zju.edu.cn, Tel/Fax: 86-579-88208596)* or Dr. Yue Gao (E-mail: gaoyue@bmi.ac.cn, Tel/Fax: 86-10-6691312)

Table of Contents (TOC)

The Fructus Meliae Toosendan induced liver injury in mice was investigated by integrating the data from miroRNA and mRNA expression profilings combined with the general toxicological assessments method.

Abstract

Fructus Meliae Toosendan (FMT, ChuanLianZi in Chinese) is recognized as an insecticidal and medicinal plant in China. A few previous study demonstrated that it can induce hepatotoxicity, however, its potential toxic compositions and their mechanism of the induction of hepatotoxicity has not been completely investigated.

In the present study, we performed an approach of integrating the data from microRNA (miRNA) and mRNA expression profilings combined with the general toxicological assessments method to investigate the FMT-induced liver injury (FMT-ILI) in mice. Changes in the body weight, serum biochemical parameters, and histopathology were observed after 9 days exposure to FMT. A total of 37 miRNAs and 931 mRNAs were differentially expressed in the liver of FMT-treated mice. By miRNA target filter and data intersection, a total of 115 mRNA targets of the identified miRNA were obtained. Ingeniuty pathway analysis showed that lipid metabolism disorders play critical roles in FMT-ILI. Results from multi-facets of the genomic profiling provided novel insights into mechanisms of FMT-ILI and contributed to a better understanding of liver pathobiology of Traditional Chinese Medicine (TCM) hepatoxicity.

Keywords: The fruit of *Melia toosendan Sieb. Et Zucc*., mRNA, microRNA, lipid metabolism, liver injury.

Introduction

As an alternative or complementary therapy, Traditional Chinese Medicine (TCM) has become more frequently used throughout the world[1]. TCM is usually perceived by general public as an efficacious treatment with few side effects, however, increasing cases have been reported that several TCM caused serious adverse reactions on patients, including liver injury[2]. Despite of considerable amount of attentions by research communities, potential mechanisms of TCM-induced liver injury remained elusive, which is partially related to unknown toxic compositions and complex toxicological modes of actions from multiple ingredients of TCM.

Fructus Meliae Toosendan (FMT) is mature fruit from *Melia Toosendan Sieb. Et.Zucc.* (ChuanLianZi in Chinese), that has long been recognized as an insecticidal and medicinal plant to treat stomach ache, cholelithiasis, cholecystitis, gastritis, mastitis, and ascariasis in China and Korea. A variety of components, including triterpenoids[3], steroids[3], and limonoids[4-6], have been described in FMT. These components displayed a wide range of biological activities *in vitro*, such as insecticidal[7, 8], anti-cancer[3, 9, 10], antimicrobial and antifeedant[8] activities. Toosendanin is the main bioactive ingredient of FMT and has been identified as a promising lead compound for treating botulism[11] and cancer[12]. Several reports had demonstrated that FMT can induce liver toxicity in both experimental animals and clinical patients[13, 14] in which inflammatory response and oxidative stress were proposed to be involved in the process[15], however, molecular mechanisms of FMT-induced liver injury (FMT-ILI) still remain largely unknown. It has been shown that majority of identified active components of FMT, including the most well studied active ingredient toosendanin, were concentrated in the ethyl acetate extracts[6]. Moreover, a previous study concluded that ethyl acetate extraction showed more serious toxicity than other extraction parts *in vivo*[16]. Therefore, we focused on FMT ethyl acetate extracts-induced liver injury in this study.

Toxicogenomics has attracted widespread attention as a promising approach to study underlying toxicological mechanisms from a systemic point of view, which reveals the relationship between toxicant exposure and alterations in genome-wide gene expression patterns[17]. This approach has been already employed to investigate toxicological effects of TCM, including liver toxicity[18, 19]. In our laboratory, we have also applied toxicogenomics as a tool to better understand the toxicity mechanisms and identify potential biomarkers for drug-induced liver injury (DILI), such as antibiotic drugs[20, 21]. For herbal-induced liver injury (HILI), several studies have focused on the influence of medicinal herbs on mRNA profiling in liver, however, only few studies have extended this approach on miRNAs expression levels. miRNAs are the family of 21–25-nucleotide small RNAs that negatively regulate gene expression at the post-transcriptional level[22]. It is estimated that at least 1/3 of human genes are regulated by miRNAs that are relative stable in a variety of tissues and body fluids. Based on this property, great attention has been attracted on miRNAs as clinical and translational biomarkers of DILI[23, 24]. Several studies have also reported that a set of

miRNAs contribute to the development of several liver diseases, such as lipid metabolism disorders, hepatitis, fibrosis, and hepatocellular carcinoma.

As miRNAs being most of the abundant regulators of mRNA, it is interesting to correlate the regulatory relationships between miRNA and its mRNA targets into the study of HILI. Since mammals miRNAs predominantly act to decrease target mRNA levels, inducing a concomitant mRNA degradation in 87% of cases[27], therefore the expression changes between miRNAs and the mRNA targets of those miRNAs can be defined as a negative correlation relationship. Study miRNA and mRNA intersections will provide more comprehensive view of the mechanisms involved in HILI.

In this study, in order to investigate the FMT-ILI, general toxicological assessments were performed, followed by mRNA and miRNA expression profilings using microarray analysis on liver samples. Furthermore, an informatics tool of IPA (Ingeniuty Pathway Analysis) was used to identify important mRNAs and miRNAs whose expression were significantly altered by FMT treatment, which would shed some light on molecular mechanisms of FMT-ILI. **Fig. 1** showed the overall research strategy and experimental design in this study. Our results demonstrated that lipid metabolism disorders play critical roles in FMT-ILI. The integrative approach with miRNA-mRNA intersection provided a comprehensive understanding of FMT-ILI.

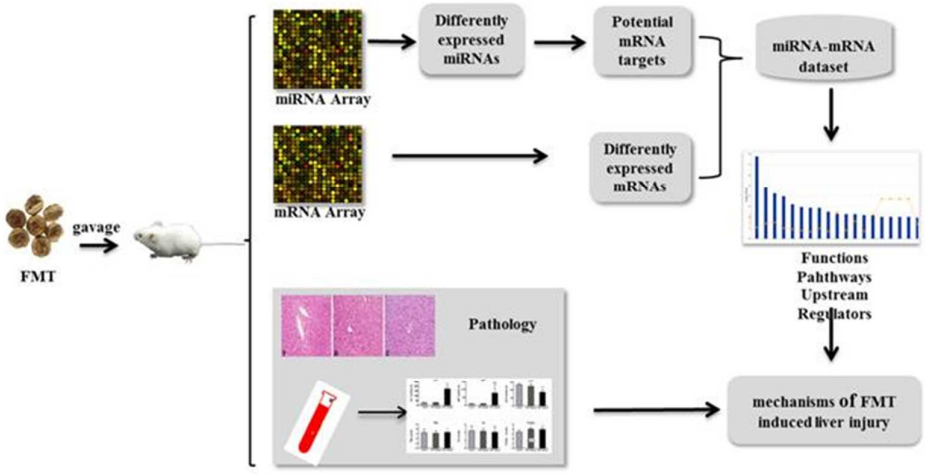

Fig. 1 Overview of the research strategy and experimental design.

Materials and methods

Preparation of the ethyl acetate extracts of FMT

FMT were purchased from Zhejiang Chinese Medical University Medicine Plant, Hangzhou, China (product lot no. 130301) and identified by associated professor Liurong Chen (College of Pharmaceutical Sciences, Zhejiang University, China). Dried FMT (23.5 kg) were soaked overnight and extracted with 95% ethyl alcohol (EtOH) (1:8, w/v) twice for 90 min. After evaporation of the EtOH, the crude extracts were suspended in deionized water and extracted with petroleum ether (PE) (1:1, v/v) and

ethyl acetate (EtOAc) (1:1, v/v), 4 times successively. Finally, 166.4 g of the ethyl acetate extracts was obtained, stored at -20 °C, and suspended with 1% sodium carboxymethyl cellulose before use. The components in the ethyl acetate extracts of FMT were investigated by high performance liquid chromatography-electrospray ionization-mass spectrometry (HPLC-ESI-MS). Toosendanin, trichilin B, trichilin I, 12-O-acetylazedarachin B, 12-O-acetylazedarachin A, trichilin H, trichilin K or its analogs, 12-O-acetyltrichilin B, and 1-O-cinnamoyltrichilinin were identified. These components all belong to limonoids. The content of toosendanin in the ethyl acetate extracts of FMT was 60.4 mg/g determined by HPLC.

Animal treatment and sample collection

Male BALB/c mice (18−20 g, Silaike Co. Shanghai, China) were housed in an environmentally controlled room at 25 ± 1 °C with a relative humidity of 50% ± 10% under a cycle of 12 h each light/dark. Food and tap water were freely accessed by the animals. The mice were administrated daily with the ethyl acetate extracts of FMT at dose levels of 20 or 40 g/kg body weight (n = 8, an equivalent amount of the crude drug) or vehicle control (n = 8, 1% sodium carboxymethyl cellulose) through oral gavage for 9 days (0.2 mL/10 g). The doses were determined by our preliminary experiments as the high dose induced obvious changes in the parameters of general toxicological assessments and low dose caused slight effects. Based on the previous studies, the LD50 of FMT in mice (82.85 g/kg)[16] and some large dose administration in clinic for humans which is equal to 26 g/kg daily for mice[28] were also considered for the dose determination. Individual body weights (BWs) was recorded every day. Orbital blood samples were obtained on the 10th day for clinical biochemical analysis. For microarray analysis, 200 mg of excised samples from the left lateral liver lobe were directly flash frozen in liquid nitrogen and used for further analysis. The remaining liver lobes were used for histopathological examinations. All sampling procedures were performed in accordance with the Guiding Principles in the Use of Animals in Toxicology and the Animal Care and Use Committee of Zhejiang University School of Medical.

Serum biochemical analysis and histopathological examinations

Whole blood samples were centrifuged at 4,000 rpm for 15 min at 4 ℃. The resulted serum was used for biochemical analysis. The parameters, including alanine transaminase (ALT), aspartate transaminase (AST), alkaline phosphatase (ALP), total bilirubin (TBIL), total cholesterol (TCHOL), and triglyceride (TG), were detected using the Cobas C8000 system (Roche Diagnostics, Germany) according to the manufacturer's instructions.

The section liver samples for histopathological examinations were fixed immediately in 10% neutral-buffered formalin for at least 24 h. The tissues were embedded in paraffin, sectioned into 4-μm thick slices, mounted on special treated slides, stained with hematoxylin and eosin, and examined by optical microscope.

RNA extraction and purification

Total RNA from the 40 g/kg FMT and vehicle control groups (n = 5, chose the first 5 mice with higher ALT levels in FMT treatment group, and randomly selected 5 mice in vehicle control group) was extracted and purified using mirVana™ miRNA Isolation Kit (Ambion, Austin, TX, US) following the manufacturer's instructions. RNA quality was inspected by an Agilent Bioanalyzer 2100 (Agilent technologies, Santa Clara, CA, US) and electrophoresis in 2% (w/v) agarose gels. Samples with RNA Integrity Number (RIN) greater than 7.0 and 28S/18S ratio greater than 0.7 were used for microarray analysis and real-time PCR. A260/A280 nm absorbance ratio of RNA samples used in this experiment consistently ranged from 1.8 to 2.0.

Microarray analysis of mRNA and miRNA expression

For the mRNA profiling, Affymetrix mouse 430 2.0 array was used according to manufacturer's instructions. The detailed description was shown in our previous study[21]. For the miRNA profiling, Agilent Mouse miRNA V19.0 was used according to manufacturer's instructions. Each slide was hybridized with 100 ng Cy3-labeled RNA using miRNA Complete Labeling and Hyb Kit (Agilent technologies, CA) in hybridization Oven (Agilent technologies, CA) at 55 °C, 20 rpm for 20 h. Slides were then washed in staining dishes (Thermo Shandon, MA) with Gene Expression Wash Buffer Kit (Agilent technologies, CA).

Microarray data analysis

The mRNA Hybridized slides were scanned by GeneChip® Scanner 3000 (Affymetrix, CA) and Command Console Software 3.1 (Affymetrix, CA) with default settings. Raw data were imported into the ArrayTrack® v.3.5.0 for further analysis. Microarray data were normalized by MAS 5.0 algorithm and were further normalized per chip to the same median intensity value of 1000. The Welch's *t*-test was employed. The cutoff for selection of differentially expressed mRNAs (DEGs) was based on a p value < 0.05 combined with absolute fold change (FC) > 2 and mean channel intensities > 250.

For the analysis of miRNA data, slides were scanned by Agilent Microarray Scanner (Agilent technologies, CA) and Feature Extraction software 10.7 (Agilent technologies, CA) with default settings. Raw data were normalized with Quantile algorithm and log2 transformed by Gene Spring Software 11.0 (Agilent technologies, CA). Only the mean intensity of miRNAs in at least one of the two groups (FMT-treated and the vehicle control groups) > 4 (log2 transformed intensity) was considered. Furthermore, the student's t-test was also performed. The cutoff for selection of differentially expressed miRNAs (DEMs) was according to a p value < 0.05 combined with FC > 1.5.

An unsupervised hierarchical clustering analysis (HCA), based on the expression levels of the DEGs and DEMs, was performed for visualizing the cluster of FMT-treated and the vehicle control samples.

Validation of microarray data by RT-PCR

The expression levels of selected DEGs and DEMs were verified by real-time reverse transcription Polymerase Chain Reaction (RT-PCR). The same total RNA was used for both microarray and RT-PCR experiments. To validate mRNA, cDNA was synthesized from 8 μg total RNA via reverse transcription with oligo-dT15 primer (Promega, USA) and SuperScript II reverse transcriptase (Invitrogen, USA). PCR reactions were carried out using QuantiFast SYBR Green PCR Kit (QIAGEN, USA) following manufacturer's instructions. miRNA RT-PCR was performed using miScript II RT Kit (QIAGEN, USA) and miScript SYBR® Green PCR Kit (QIAGEN, USA) for reverse transcription and real time-PCR analysis, respectively. The Ct value of each sample was standardized to the selected house-keeping gene (GAPDH and U6 for mRNA and miRNA, respectively). Experiments were conducted in technical triplicates. The sequences of primer for mRNA and miRNA were listed in Supplementary Table S1. All RT-PCR reactions were performed using the real-time thermal cycler (Mastercycler realplex 4, Eppendorf, USA).

miRNA targets prediction

The DEMs were loaded into IPA (http://www.ingenuity.com) for their corresponding target information. The IPA "miRNA target filter analysis" was performed with three separate algorithms (TargetScan, TarBase and miRbase) to predict potential relationships between miRNA and its mRNA targets. Detailed description about this procedure can be found in the online repository of IPA.

Ingeniuty Pathway Analysis

Both of the DEGs and of DEMs were loaded into IPA. An intersection between DEGs and mRNA targets of DEMs dataset was generated as the miRNA-mRNA intersection dataset. The tox analysis function in IPA was performed to this dataset for biofunctions, canonical pathways and upstream regulators analyses. A right-tailed fisher's exact test was used to calculate a *p* value to determine the statistical significance of association between our selected objects and the biological functions or related pathways within IPA. The *p* values of the pathways were reported as a range as there were several biofunction branches for one pathway and the *p* value of each biofunction branch was given. A z-score algorithm was applied as to make predictions of upstream regulators. The z-score algorithm is designed to produce either a prediction of activation (the z-score is ≥ 2) or inhibition (the z-score is ≤ -2), or no prediction based on the default setting in IPA.

Statistical analysis

Statistical differences between the FMT treated and control groups were examined by two-sided Student's t-test. Statistical differences between these two groups of the data from body weight and serum biochemical parameter were determined by one-way ANOVA followed by Bonferroni Post Test. p-value < 0.05 was considered to

be significant.

Results

Oral FMT treatment induced liver injury in mice

First, we evaluated the general toxicological effects of FMT on mice at two dose levels (low: 20 g/kg and high: 40 g/kg) after nine consecutive days of oral gavage. During the administration period, several abnormal symptoms appeared in mice dosed with 40 g/kg FMT, including emaciation, poor mental state and withered hair color. One mouse in this group was dead on the fifth day. Compared with control group, body weights of 40 g/kg FMT group decreased progressively during the 9-day treatment and significant difference was observed since the fourth day (**Fig. 2a**). The results of serum biochemical analysis in control and FMT groups at day 10 were summarized in **Fig. 2b**. Serum ALT and AST are the golden standard biomarkers for liver function and damage assessment[28]. In this study, serum ALT activity from the 40 g/kg FMT treated mice increased approximately three times compared with control group, whereas the AST showed more robust increase to nearly 5 times. Moreover, the activity of ALP decreased significantly ($p < 0.01$) as well as moderate increase of TCHOL level detected in 40 g/kg FMT treatment ($p < 0.05$), compared with the control group. In addition, there was no statistical significant alterations observed on the level of TG and TBIL between 40 g/kg FMT treated and control groups. Furthermore, widespread hydropic degeneration of hepatocytes was observed in the livers of 40 g/kg FMT-treated mice in histopathological examinations (**Fig. 2c**). Additionally, no obvious signs of toxicity were observed in these general toxicological assessments in 20 g/kg FMT-treated group (**Fig. 2a-c**), expect the moderate hydropic degeneration of hepatocytes detected in histopathological examinations, indicating low dose level of FMT was relatively safe to the animals.

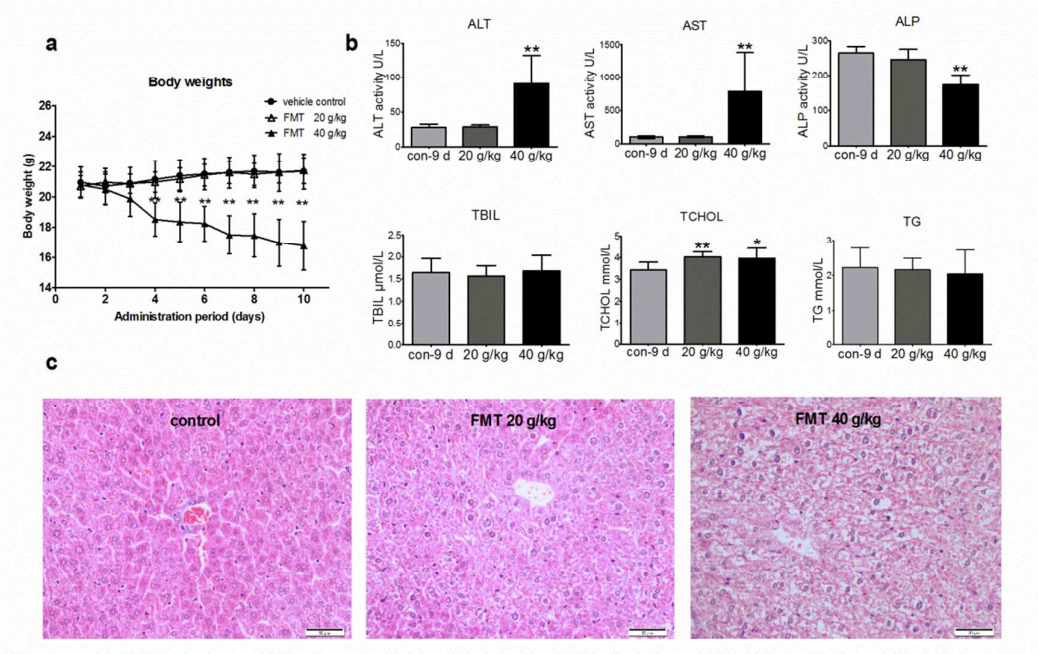

Fig. 2 The effects of 9-day FMT treatment on the general toxicological parameters (n = 7 or 8). (a) The body weight. (b) The selected serum biochemical parameters. (c) Photomicrographs of liver tissues with hematoxylin and eosin staining. The magnification used was ×400. The scale bar is 50 μm. The images are representative of at least three independent sections. Data were presented as mean ± SD. Con in Fig. 2b indicates the control group. Statistical analysis was performed using one-way ANOVA followed by Bonferroni Post Test. * $p < 0.05$, ** $p < 0.01$, compared with control group.

Differentially expressed mRNAs (DEGs)

Data analysis of mRNA expression profiling identified that 931 out of 45101 mRNAs were differentially expressed (593 up-regulated, 338 down-regulated) after 40 g/kg FMT treatment. Based on these DEGs, the results of HCA revealed a clear separation of two major clusters, 40 g/kg FMT treatment group and control group (**Fig. 3a**). Results showed that a plenty of lipid and xenobiotics metaboloism related genes were deregulated by 40 g/kg FMT treatment. For instance, the gene expressions of Fmo3 and cytochrome P450 (Cyp450) family were significantly increased upon FMT treatment (Details of mRNA expression data were provided in Supplementary Table S2), suggesting potential involvement of drug metabolic enzymes in the toxicological effects of FMT. Among them, 3 genes belonging to the Cyp4a subfamiliy were detected, including *Cyp4a14*, *Cyp4a12a* and *Cyp4a10*. They were dereguleted by 13.99-, 7.17-, and 32.57-fold, respectively. In addition, the expression of elovl3 which catalyzes the initial and rate-controlling condensation reaction to synthesis very long chain fatty acid[29] was found to be significantly decreased about 21-fold in FMT treatment group.

Differentially expressed miRNAs (DEMs)

Among the 1249 miRNA probes examined in liver samples of 40 g/kg FMT treated mice, 37 miRNAs (21 up-regulated, and 16 down-regulated) were significantly differentially altered in comparison with control group. HCA on these DEMs also revealed two major clusters: control group and FMT-treated group (**Fig. 3b**). Since we were interested in downstream effects of miRNAs, those miRNAs with target information available were focused in further analysis. As the results, a total of 12 miRNAs were selected, including 6 miRNAs up-regulated (miR-574-3p, miR-3082-5p, miR-466i-3p, miR-706, miR-574-5p, and miR-467f) and 6 miRNAs down-regulated (miR-877-5p, miR-290-5p, miR-3102-5p, miR-3960, miR-296-5p, and miR-1249-3p) in 40 g/kg FMT-treated mice.

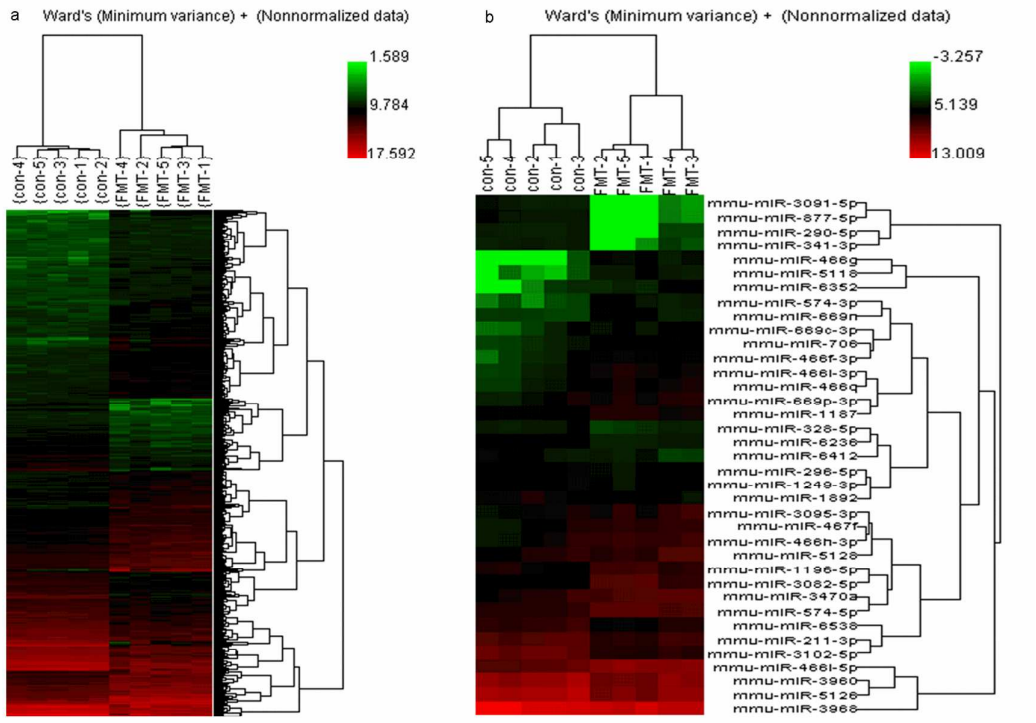

Fig. 3 Hierarchical cluster analysis (HCA) of the data from mRNA and miRNA expression profiles of 40 g/kg FMT treatment (n = 5). (a) HCA of the DEGs (differentially expressed mRNAs) in the liver in response to 40 g/kg FMT treatment. (b) HCA of the DEMs (differentially expressed miRNAs) in the liver in response to 40 g/kg FMT treatment.

Validation of mRNA and miRNA expression

In order to validate mRNA microarray results, we performed real-time RT-PCR on selected genes. Ten mRNAs, including *Fmo3*, *Cyp2b9*, *Cyp4a14*, *Cyp4a12a*, *Gadd45*, *Elovl3*, *Igfbp1*, *Ugt2b38*, *Slco1a1*, and *Hsd3b5* exhibited a high correlation with primary microarray results. It highlighted the reliability of the microarray experiment (**Fig. 4a**). These stably dysregulated candidate mRNAs could have the potential to serve as diagnostic biomarkers for FMT-ILI. To validate the results from miRNA microarray, three miRNAs were selected and their expression levels in liver tissue

were examined by RT-PCR, which also showed a high correlation with primary microarray results (**Fig. 4b**).

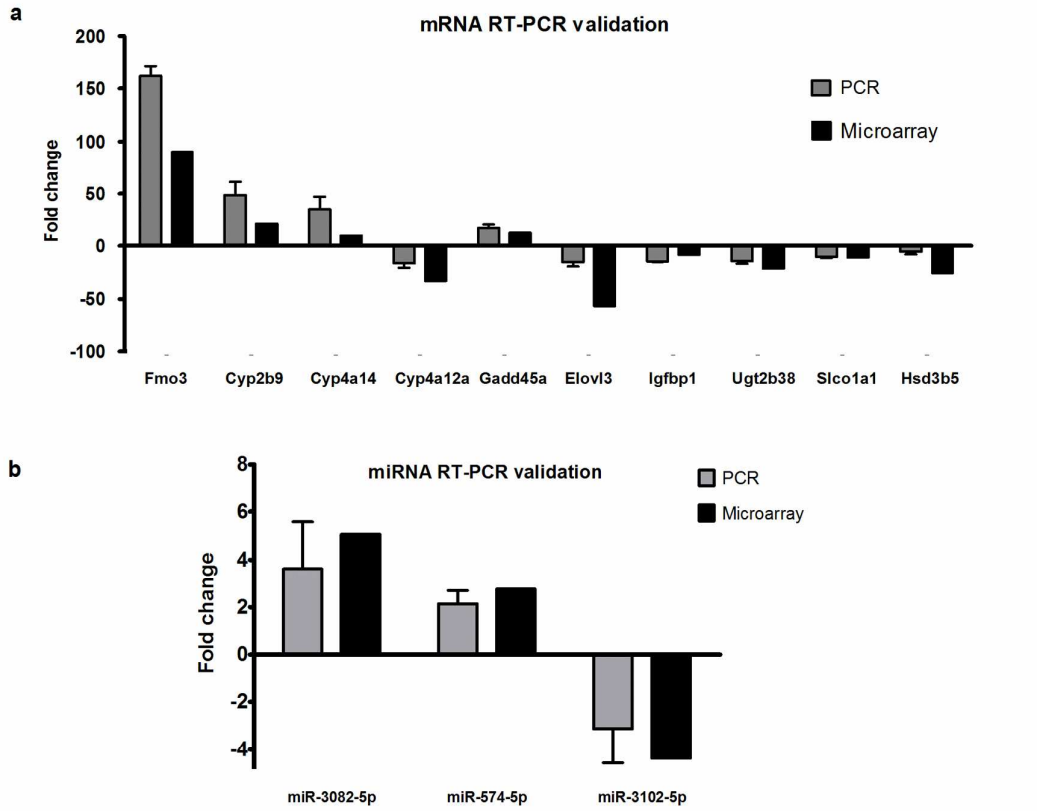

Fig. 4 Validation of the microarray results by quantitative RT-PCR. (a) The dysregulated mRNAs in response to 40 g/kg FMT treatment, including *Fmo3*, *Cyp2b9*, *Cyp4a14*, *Cyp4a12a*, *Gadd45*, *Elovl3*, *Igfbp1*, *Ugt2b38*, *Slco1a1*, and *Hsd3b5*. (b) Validation of the dysregulated miRNAs in response to 40 g/kg FMT treatment, including miR-3082-5p, miR-574-5p, and miR-3102-5p. The fold change of FMT-treated group compared to control group in RT-PCR experiments was calculated by the $2^{-\Delta\Delta CT}$. Black bars indicate microarray data. Gray bars indicate mean fold change (± SD) derived from 3 independent experiments performed in duplicate of RT-PCR experiments.

miRNA-mRNA interactions

According to miRNA target filter analysis, the 12 identified miRNAs were matched with 5136 target mRNAs. After taking the information about DEGs from mRNA profile in account, 11 modulated miRNAs were coherently linked with 194 target mRNAs. Furthermore, among these target mRNAs, a number of 115 mRNAs showed an opposite expression trend compared with corresponding miRNA. This regulation relationship was shown in **Fig. 5**. In the 11 miRNAs, miR-296-5p regulated the largest number of mRNA (46 genes). Additionally, the overlaps between the downstream target mRNAs of two miRNAs were observed. For instance, *Tmem218* and *Igfbp5*

were the potential targets both of miR-3102-5p and miR-296-5p.

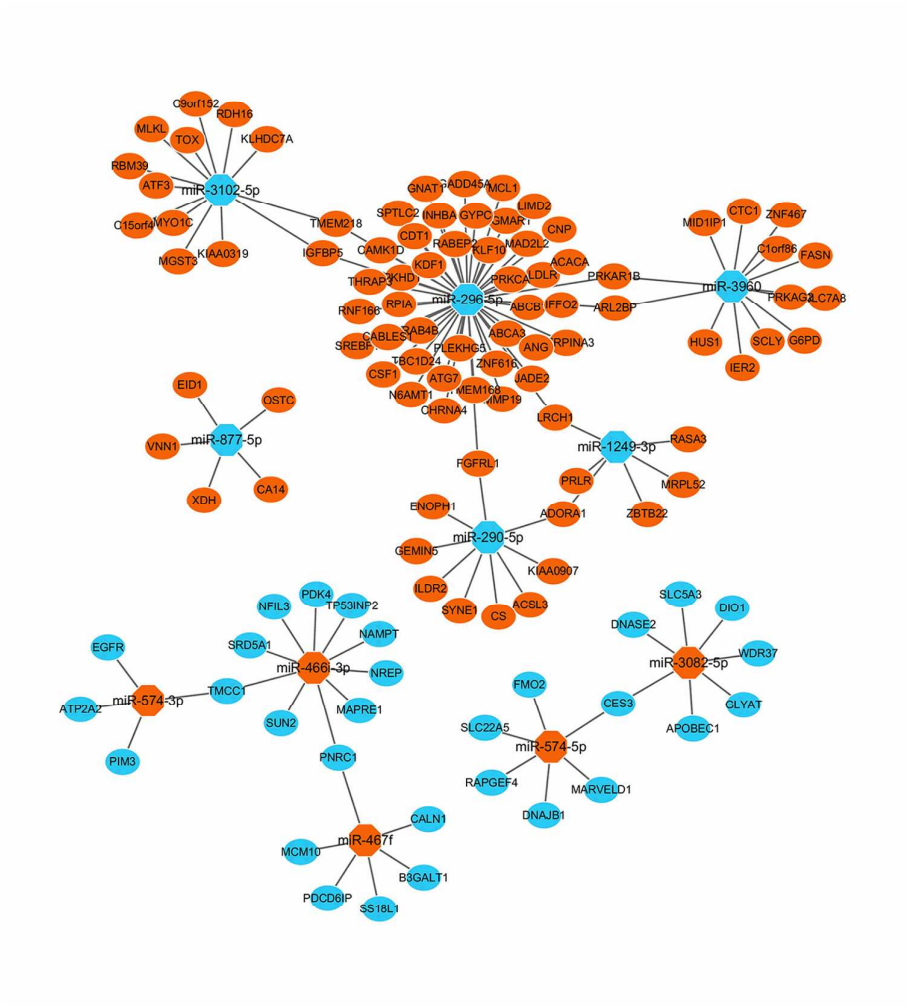

Fig. 5 The regulation relationship of the 11 miRNAs and 115 target mRNAs in 40 g/kg FMT-treated liver tissue. The 11 miRNAs were the DEMs in the liver in response to 40 g/kg FMT treatment. The 115 mRNAs were the DEGs in the liver in response to 40 g/kg FMT treatment, which also belonged to the target mRNAs of these 11 miRNAs mentioned above with opposite expression trend compared with corresponding miRNA. The orange color means upregulation, which compared to control group. The blue color indicates downregulation, compared to control group.

Functional and pathway analysis of data from established DEGs-DEMs

The 115 target mRNAs established a DEGs-DEMs dataset for functional and pathway analysis. The tox analysis function in IPA was performed to this dataset for biofunctions, canonical pathways and upstream regulators analyses. By using IPA tox analysis, we identified “molecular and cellular functions” were likely to alter in the liver of FMT-treated group (Table 1). The overrepresented molecular and cellular functions were associated to lipid metabolism, molecular transport, small molecule biochemistry, cellular development, as well as cell death and survival. The

hepatotoxicity induced by FMT treatment may related to liver cholestasis, liver steatosis, liver damage, liver inflammation/hepatitis, and liver necrosis/cell death predicted by IPA.

Additionally, top 10 canonical pathways and top 10 tox lists are determined by statistical significance and listed in **Fig. 6**. This analysis showed that most of the pathways or tox lists were involved in metabolic functions, especially lipid and xenobiotics metaboloism related pathways, and these pathways are meditated by drug and xenobiotic related nuclear receptors, such as PXR, LXR, CAR. Hepatic cholestasis pathway was also found dysregulated with involvement of 5 important genes (*Abcb1*, *Srebf1*, *Prkar1b*, *Prkag2*, and *Prkca*). These canonical pathways revealed the dysfunction of liver metabolic function upon FMT treatment.

Table 1.Top 5 biological functions predicted by IPA to be regulated by these 115 significantly changed mRNAs, targets of the significantly changed miRNAs.

Name	p-value[a]	Number of genes involved
Molecular and Cellular Functions		
Lipid Metabolism	2.48E-09 - 5.52E-03	37
Molecular Transport	2.48E-09 -5.52E-03	44
Small Molecule Biochemistry	2.48E-09 -5.52E-03	48
Cellular Development	1.11E-06 -5.52E-03	49
Cell Death and Survival	1.31E-06 - 5.52E-03	46
Hepatotoxicity		
Liver Cholestasis	1.98E-03 -4.33E-02	5
Liver Steatosis	2.36E-03 - 1.29E-01	6
Liver Damage	5.52E-03 - 5.09E-01	3
Liver Inflammation/Hepatitis	5.52E-03 - 2.36E-01	3
Liver Necrosis/Cell Death	7.59E-03 - 7.59E-03	4

[a]The *p* values of the pathways were reported as a range, because there were several biofunction branches for one pathway and the *p* value of each biofunction branch was given.

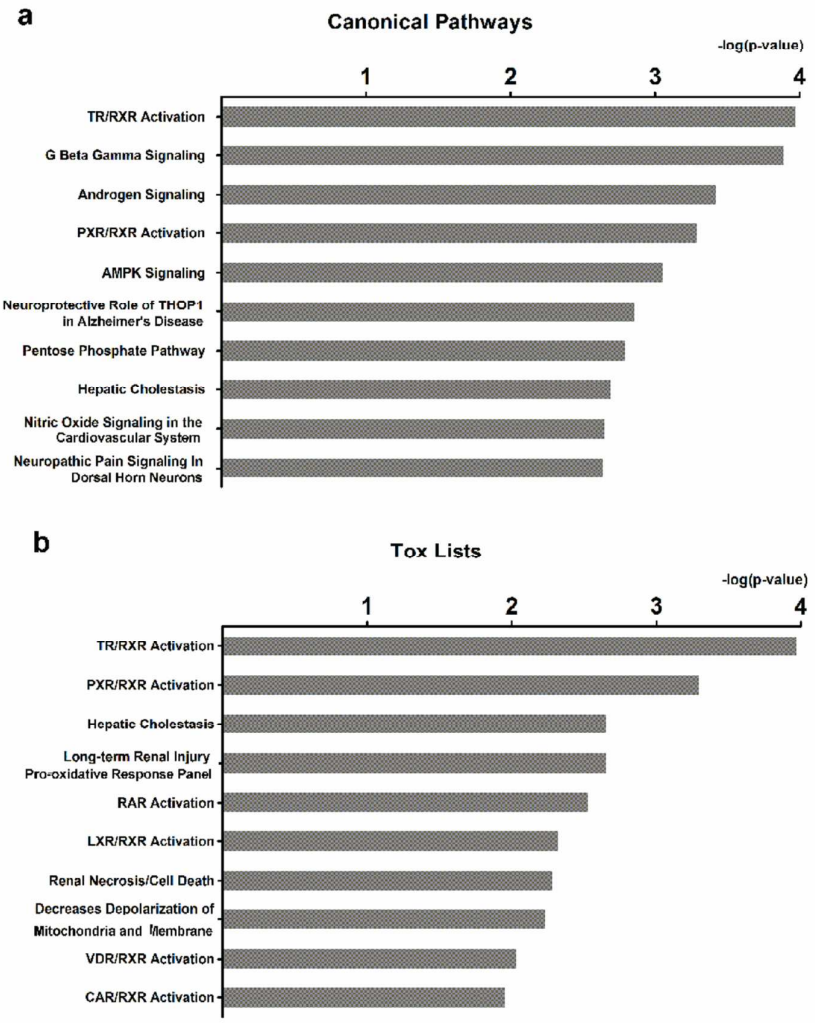

Fig. 6 The functional and pathway analysis of the DEGs-DEMs dataset. The DEGs-DEMs dataset referred to the 11 miRNAs and 115 target mRNAs mentioned above. (a) Top 10 canonical pathways of the DEGs-DEMs dataset conducted by IPA. (b) Top 10 tox lists of the DEGs-DEMs dataset performed by IPA.

Finally, the Upstream Regulator Analysis provided an insight into upstream regulatory molecules that potentially modulate target genes. A total of 22 regulators were identified to be activated or inhibited with an absolute value of Z-score > 2 (**Fig. 7**). The enrichment analysis showed significant associations of upstream regulators with functions related to lipid homeostasis, including SREBP1, SREBP2, NR1H3, INSIG1, INSIG2, ~~and~~ CYP7A1, etc. Particularly, the mRNA expression level of SREBF1 was up-regulated 4.60-fold in the mRNA microarray screening phase. In addition, the growth factors, such as IFG1 and EGF, regulating the cell proliferation and differentiation, were activated as well at mRNA level, which then has a potential risk to develop liver hyperplasia/hyperproliferation.

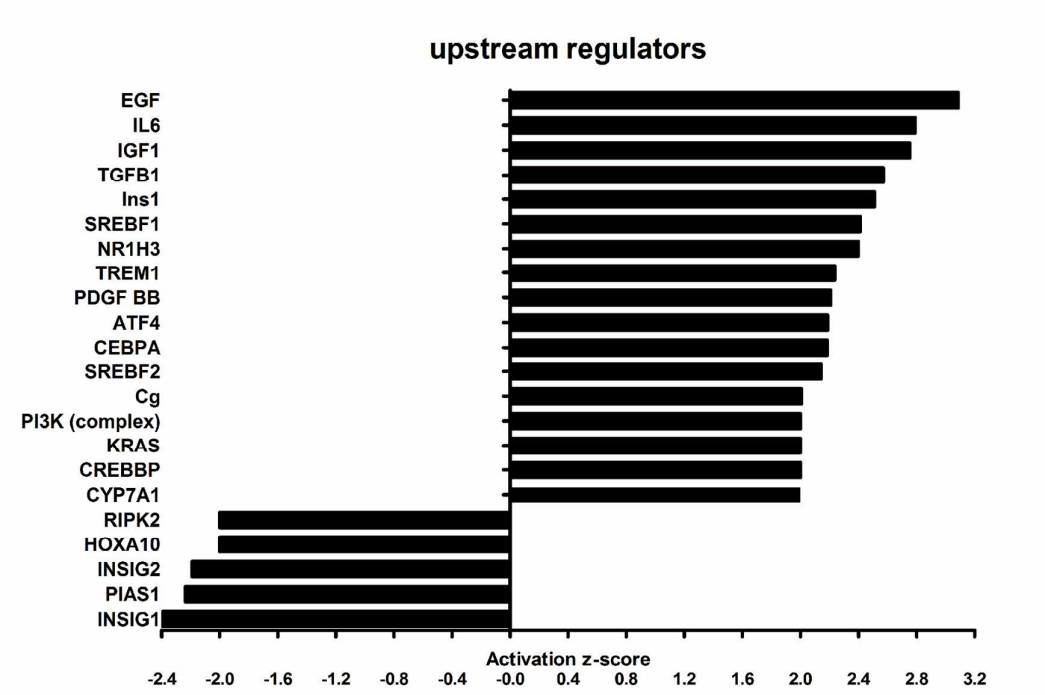

Fig. 7 The 22 upstream regulatory molecules for the 115 target mRNAs from the DEGs-DEMs dataset revealed by Upstream Regulator Analysis in IPA.

Discussion

Although FMT has been known as a hepatotoxic drug, the molecular mechanisms of FMT-ILI has not been well studied, which greatly limits the safe application of this medicinal TCM. Therefore, in this study, we aimed to identify important molecular processes in FMT-ILI based on corresponding the mRNA and miRNA expression using toxicogenomic approaches. As the evidences from general toxicological results, multiple phenotypes of liver injury were detected in 40 g/kg FMT treatment group (**Fig. 2a-c**). Moreover, microarray analysis revealed that a number of mRNA and miRNA were modulated in the progress of FMT-ILI. We identified 37 miRNAs were dysregulated in liver tissue, indicating the important role of miRNA function in FMT-ILI. At the same time, 931 mRNAs were dysregulated in the same liver tissue.

In mRNA expression profiling, results revealed robust drug-metabolizing enzymes were involved in the progress of detoxification response. The CYP450 superfamily that encodes isoforms that metabolize drugs and xenobiotics are participated in about 75% of the enzymatic reactions involved in drug metabolism. They are considered to be broadly studied hepatotoxic biomarkers. In our study, several CYP450 superfamily genes were also identified in DEGs, including 11 of them up-regulated and 7 of them down-regulated (Supplementary Table S2). Among them, *Cyp7a1* encodes the rate limiting enzyme that catalyzes the conversion of cholesterol into bile acids, thus plays a critical role in the control of cholesterol

homeostasis; the enzymes coding by *Cyp4a14*, *Cyp4a12a*, and *Cyp4a10* function as catalyzing microsomal hydroxylation of fatty acids, and inducting the CYP4A which is closely related to the fatty liver disease[30]. Another representative drug-metabolizing enzyme up-regulated in the FMT treatment was Fmo3. Fmo3 is a phase I drug-metabolizing enzymes that functions somewhat similar to CYP450, but it is considered to be a non-inducible metabolizing enzymes that involved in the oxygenation of sulfur-containing endogenous substrates. Products of *Fmo3* are considered to be nontoxic. A recent study showed that *Fmo3* may biologically play a role in autoprotection in APAP-induced hepatotoxicity in female mice[31]. Our data may indicate the protective role of *Fmo3* against FMT-ILI as well. In addition, the expression of elovl3 was also significantly decreased in FMT treatment group. Previous study showed that knockdown of *Elovl3* reduced fatty acid biosynthesis, adipogenesis, and lipolysis along with a reduction in the level of intracellular triglycerides[32]. Thus, we deduced that lipid metabolism disorders may play an important role in FMT-ILI.

Since miRNAs represent the most abundant class of mRNA expression regulators, we integrated these two microarray data to unveil mechanisms of FMT-ILI, as well as revealing the regulatory relationship between mRNAs and miRNAs. As liver is an essential metabolic organ, the integrated of mRNA and miRNA expression data in this study revealed lipid metabolism disorder may play a critical role in FMT-ILI. This is consistent with a study which revealed an increase in intracytoplasm lipid droplets in liver tissues after FMT treatment in rats[33]. In our study, there were total 37 modulated mRNA targets related to lipid metabolism (Table 1). The enrichment analysis of mRNA targets revealed that the liver toxicity-induced by FMT were mainly related to liver cholestasis and steatosis. Lipid and xenobiotics metaboloism related nuclear receptors were also involved in FMT-ILI (**Fig. 6**). Increasing number of studies demonstrated that nuclear receptors are involved in the development of many liver diseases including liver fibrosis, hepatic lipid/glucose metabolism and fatty liver disease[34]. The retinoid X receptor (RXR) acts as the dimerization partner for type II nuclear receptors[35], including farnesoid X receptor (FXR), liver X receptor (LXR), pregnane X receptor (PXR). This partnership mediates transcriptional control and involved in a diversity of physiological processes ranging from cell proliferation to lipid metabolism. Pregnane X receptor (PXR) is an important regulator of drug excretion and metabolism. The activated PXR in conjunction with RXR plays a key role in drug metabolism by inducing the CYP450 family of enzymes. Our research also predicted several activated upstream regulators of the dysregulated genes which were related to lipid metabolism. For example, SREBP1 plays a crucial role in the regulation of hepatocyte lipid homeostasis. Studies found activation of SREBP-1 by ethanol feeding was associated with increased expression of hepatic lipogenic genes as well as the accumulation of triglyceride in the livers[36]. Taken together, all nuclear receptors related canonical pathways and upstream regulators mentioned above unequivocally have been shown to function as key regulators of pathways in lipid

metabolism and homeostasis, indicating the disorders in lipid metabolism play a critical role in FMT-ILI.

At the same time, disturbance of carbohydrate metabolism was also observed as involvement of the Pentose Phosphate Pathway (PPP, **Fig. 6**). As an alternative pathway of glucose metabolism, the PPP is responsible for producing nicotinamide adenine dinucleotide phosphate (NADPH) and ribose-5-phosphate. NADPH is needed in many anabolic pathways, such as lipid synthesis, fatty acid chain elongation and cholesterol synthesis. An increase demand for NADPH production through the PPP is closely related to antioxidant defense reactions[37]. Induction of genes involved in the PPP may be the result of disorders of lipid homeostasis and oxidative stress in FMT-ILI.

~~Specific miRNA signatures have been identified in the etiology of various liver diseases.~~ In addition, a well studied miRNA is miR-122, which is a liver-enriched miRNA accounting for approximately 70% of total hepatic miRNAs. Inhibition of miR-122 expression in mice leads to a down-regulation of lipid metabolism and cholesterol, specifically down-regulating the key enzyme phosphomevalonate kinase. The previous study suggested that the serum miR-122 was at least as informative as the ALT in humans for acetaminophen (APAP)-induced liver injury[38]. In our study, however, the expression level of miR-122 in treated mice did not show significant difference in FMT group compared with control group, which may be related to the usage of liver tissue for miRNA microarray. A recent study has demonstrated that damaged hepatocytes contribute to the increase in circulating miR-122 levels, while dysregulation of hepatic miR-122 levels requires multiple hits[39]. Similar to our observation, the expression level of miR-574[40], miR-296-5p[41], miR-877-5p[42] have found dysregulated in various liver disease models as well. More efforts should be carried out to characterize functions of these miRNAs.

Conclusions

In conclusion, we have demonstrated a strong response in mRNA and miRNA in the livers of mice exposed to FMT by oral gavage. As integrated analysis of the intersection of DEGs and DEMs, the present study details the molecular mechanisms underlying FMT-ILI. Lipid metabolism disorders may play an important role in FMT-ILI as well as the oxidative stress. However, to elucidate the exact mechanism, these changes need to be further confirmed by measuring the protein and metabolite levels. Moreover, further study in miRNAs functions and its target genes are urgently needed to better use miRNAs as toxicogenomic tools. Although additional work needed, the findings from this study provide insight into the mechanisms of FMT-ILI by multi-facets of the transcriptome, which can be used as a tool to better understand the pathobiology of HILI.

Acknowledgments

This work was financially supported by the National Natural Science Foundation of China (No. 81173465 & 81403275), the Program for New Century Excellent Talents in University (NCET-12-0488), and the Specialized Research Fund for the Doctoral Program of Higher Education (No. 20120101120137).

Notes and references

† Electronic Supplementary Information (ESI) available: sequences of primer for mRNA, sequences of primer for miRNA, lists of genes up-regulated upon FMT-treatment, lists of genes down-regulated upon FMT-treatment.

1. W. L. Hsiao and L. Liu, *Planta Med*, 2010, **76**, 1118-1131.
2. R. Teschke, A. Wolff, C. Frenzel and J. Schulze, *Aliment Pharm Therap*, 2014, **40**, 32-50.
3. S. B. Wu, J. J. Su, L. H. Sun, W. X. Wang, Y. Zhao, H. Li, S. P. Zhang, G. H. Dai, C. G. Wang and J. F. Hu, *J Nat Prod*, 2010, **73**, 1898-1906.
4. Q. Zhang, J. K. Li, R. Ge, J. Y. Liang, Q. S. Li and Z. D. Min, *Fitoterapia*, 2013, **90**, 192-198.
5. Y. Zhang, C. P. Tang, C. Q. Ke, X. Q. Li, H. Xie and Y. Ye, *Phytochemistry*, 2012, **73**, 106-113.
6. T. Akihisa, X. Pan, Y. Nakamura, T. Kikuchi, N. Takahashi, M. Matsumoto, E. Ogihara, M. Fukatsu, K. Koike and H. Tokuda, *Phytochemistry*, 2013, **89**, 59-70.
7. C. Coria, W. Almiron, G. Valladares, C. Carpinella, F. Luduena, M. Defago and S. Palacios, *Bioresour Technol*, 2008, **99**, 3066-3070.
8. M. C. Carpinella, M. T. Defago, G. Valladares and S. M. Palacios, *J Agric Food Chem*, 2003, **51**, 369-374.
9. N. G. Ntalli, F. Cottiglia, C. A. Bueno, L. E. Alche, M. Leonti, S. Vargiu, E. Bifulco, U. Menkissoglu-Spiroudi and P. Caboni, *Molecules*, 2010, **15**, 5866-5877.
10. T. Kikuchi, X. Pan, K. Ishii, Y. Nakamura, E. Ogihara, K. Koike, R. Tanaka and T. Akihisa, *Biol Pharm Bull*, 2013, **36**, 135-139.
11. Y. L. Shi and Z. F. Wang, *Acta Pharmacol Sin*, 2004, **25**, 839-848.
12. B. Zhang, Z. F. Wang, M. Z. Tang and Y. L. Shi, *Invest New Drugs*, 2005, **23**, 547-553.
13. M. F. Yuen, S. Tam, J. Fung, D. K. Wong, B. C. Wong and C. L. Lai, *Aliment Pharmacol Ther*, 2006, **24**, 1179-1186.
14. X. P. Zhao, Z. W. Ge, Y. F. Zhang, X. H. Lan and B. L. Zhang, *Zhongguo Zhong Yao Za Zhi*, 2013, **38**, 1820-1822.
15. R. M. J. H. S. Y. Qi, *Zhongguo Zhong Yao Za Zhi*, 2008, **33**, 2045-2047.
16. L. Cheng, Y. Lei, Y. Y. Liang, D. X. Tang, L. Huang and Z. H. Tan, *Zhong Yao Cai*, 2007, **30**, 1276-1279.
17. E. F. Nuwaysir, M. Bittner, J. Trent, J. C. Barrett and C. A. Afshari, *Mol Carcinog*, 1999, **24**, 153-159.
18. J. Wang, Z. Jiang, J. Ji, X. Wang, T. Wang, Y. Zhang, T. Tai, M. Chen, L. Sun, X. Li

and L. Zhang, *Food Chem Toxicol*, 2013, **58**, 495-505.
19. Y. W. Su, X. Chen, Z. Z. Jiang, T. Wang, C. Wang, Y. Zhang, J. Wen, M. Xue, D. Zhu, Y. Zhang, Y. J. Su, T. Y. Xing, C. Y. Zhang and L. Y. Zhang, *PLoS One*, 2012, **7**, e37395.
20. X. Lu, Y. Tian, X. Lian, Y. Jin, T. Jin, Q. Zhao, B. Hu, X. Shen and X. Fan, *Food Chem Toxicol*, 2014, **65**, 343-355.
21. X. Lu, B. Hu, L. Shao, Y. Tian, T. Jin, Y. Jin, S. Ji and X. Fan, *Food Chem Toxicol*, 2013, **55**, 444-455.
22. L. He and G. J. Hannon, *Nat Rev Genet*, 2004, **5**, 522-531.
23. Y. Wang, T. Chen and W. Tong, *Biomark Med*, 2014, **8**, 161-172.
24. X. Yang, Z. Weng, D. L. Mendrick and Q. Shi, *Toxicol Lett*, 2014, **225**, 401-406.
25. C. Esau, S. Davis, S. F. Murray, X. X. Yu, S. K. Pandey, M. Pear, L. Watts, S. L. Booten, M. Graham, R. McKay, A. Subramaniam, S. Propp, B. A. Lollo, S. Freier, C. F. Bennett, S. Bhanot and B. P. Monia, *Cell Metab*, 2006, **3**, 87-98.
26. J. Kota, R. R. Chivukula, K. A. O'Donnell, E. A. Wentzel, C. L. Montgomery, H. W. Hwang, T. C. Chang, P. Vivekanandan, M. Torbenson, K. R. Clark, J. R. Mendell and J. T. Mendell, *Cell*, 2009, **137**, 1005-1017.
27. H. Guo, N. T. Ingolia, J. S. Weissman and D. P. Bartel, *Nature*, 2010, **466**, 835-840.
28. Q. I. Shuang-yan, X. Yan-hong and J. Ruo-min, *LISHIZHEN MEDICINE AND MATERIA MEDICA RESEARCH*, 2008, **19**, 2694-2696.
29. A. Jakobsson, R. Westerberg and A. Jacobsson, *Prog Lipid Res*, 2006, **45**, 237-249.
30. J. P. Hardwick, D. Osei-Hyiaman, H. Wiland, M. A. Abdelmegeed and B. J. Song, *PPAR Res*, 2009, **2009**, 952734.
31. S. Rudraiah, P. R. Rohrer, I. Gurevich, M. J. Goedken, T. Rasmussen, R. N. Hines and J. E. Manautou, *Toxicol Sci*, 2014, **141**, 263-277.
32. T. Kobayashi and K. Fujimori, *Am J Physiol Endocrinol Metab*, 2012, **302**, E1461-E1471.
33. Q. I. Shuangyan, Y. Gu, J. Ruo Min, L. Hongjie and M. Caixia, *China Journal of Chinese Meteria Medica*, 2009, **34**, 2966-2968.
34. M. Wagner, G. Zollner and M. Trauner, *Hepatology*, 2011, **53**, 1023-1034.
35. P. Lefebvre, Y. Benomar and B. Staels, *Trends Endocrinol Metab*, 2010, **21**, 676-683.
36. M. You, M. Fischer, M. A. Deeg and D. W. Crabb, *J Biol Chem*, 2002, **277**, 29342-29347.
37. K. Smolkova and P. Jezek, *Int J Cell Biol*, 2012, **2012**, 273947.
38. L. P. Starkey, J. Dear, V. Platt, K. J. Simpson, D. G. Craig, D. J. Antoine, N. S. French, N. Dhaun, D. J. Webb, E. M. Costello, J. P. Neoptolemos, J. Moggs, C. E. Goldring and B. K. Park, *Hepatology*, 2011, **54**, 1767-1776.
39. S. Bala, J. Petrasek, S. Mundkur, D. Catalano, I. Levin, J. Ward, H. Alao, K. Kodys and G. Szabo, *Hepatology*, 2012, **56**, 1946-1957.
40. O. Cheung, P. Puri, C. Eicken, M. J. Contos, F. Mirshahi, J. W. Maher, J. M. Kellum, H. Min, V. A. Luketic and A. J. Sanyal, *Hepatology*, 2008, **48**, 1810-1820.
41. S. C. Cazanave, J. L. Mott, N. A. Elmi, S. F. Bronk, H. C. Masuoka, M. R. Charlton and G. J. Gores, *J Lipid Res*, 2011, **52**, 1517-1525.

42. A. Wojcicka, M. Swierniak, O. Kornasiewicz, W. Gierlikowski, M. Maciag, M. Kolanowska, M. Kotlarek, B. Gornicka, L. Koperski, G. Niewinski, M. Krawczyk and K. Jazdzewski, *Int J Biochem Cell Biol*, 2014, **53**, 208-217.

80x21mm (300 x 300 DPI)